

Hard rods in a cylindrical pore: the nematic-to-smectic phase transition

Szabolcs Varga*

Institute of Physics and Mechatronics, University of Pannonia, PO Box 158, Veszprém, H-8201 Hungary

Yuri Martínez-Ratón†

*Grupo Interdisciplinar de Sistemas Complejos (GISC), Departamento de Matemáticas,
Escuela Politécnica Superior, Universidad Carlos III de Madrid,
Avenida de la Universidad 30, E-28911, Leganés, Madrid, Spain*

Enrique Velasco‡

*Departamento de Física Teórica de la Materia Condensada,
Instituto de Ciencia de Materiales Nicolás Cabrera and Condensed Matter Physics Center (IFIMAC),
Universidad Autónoma de Madrid, E-28049 Madrid, Spain*

The effect of cylindrical confinement on the phase behaviour of a system of parallel hard rods is studied using Onsager's second virial theory. The hard rods are represented as hard cylinders of diameter D and length L , while the cylindrical pore is infinite with diameter W . The interaction between the wall and the rods is hard repulsive, and it is assumed that molecules are parallel to the surface of the pore (planar anchoring). In very narrow pores ($D < W < 2D$), the structure is homogeneous and the system behaves as a one-dimensional Tonks gas. For wider pores, inhomogeneous fluid structures emerge because of the lowering of the average excluded volume due to the wall-particle interaction. The bulk nematic-smectic A phase transition is replaced by a transition between inhomogeneous nematic and smectic A phases. The smectic is destabilized with respect to the nematic for decreasing pore width; this effect becomes substantial for $W < 10D$. For $W > 100D$, results for bulk and confined fluids agree well due to the short range effect of the wall ($\sim 3 - 4D$).

PACS numbers: 61.30.Pq, 64.70.M-, 47.57.J-

I. INTRODUCTION

Confined liquid crystals have received considerable experimental and theoretical attention over the past decades due to their fundamental and technological importance. Liquid crystals are in contact with surfaces in many devices such as liquid-crystal (LC) displays, optical shutters and LC thermometers. In these systems it is very important to know the effect of geometrical confinement, surface roughness and particle-surface interactions on the ordering properties of LC materials [1]. Flat and curved surfaces, confinement between parallel surfaces, tubular pores, nanochannels and porous materials are just a few examples where the phase behaviour of the LCs is modified [2–10]. Several phenomena have been observed in confined LCs such as surface phase transitions [11], capillary nematization [12], layering transitions [13] and suppression of phase transitions [14, 15]. In addition to calamitic LCs, the ordering properties of discotic LCs have also been examined in the presence of different confinements [16, 17]. Even binary mixtures of plates and rods have been studied at a single wall and in a slit pore [18].

The objective of our work is to examine the effect of

the cylindrical confinement on the phase behaviour and structural properties of parallel hard cylinders, assuming that the cylinders are parallel to the surface of the pore (planar anchoring) with their axes pointing along the cylinder axis. It has been found that a bulk system of parallel hard cylinders has three different phases, namely, nematic, smectic A and solid [19, 20]. Here we focus only on the nematic and smectic A (hereafter called simply 'smectic') phases, while the solid phase is left for future studies. We use the well-known Onsager second virial theory [21, 22] which gives reasonable results for the nematic and smectic phases of parallel hard rods [23]. In our previous work we have shown that Onsager theory can be applied successfully to study the nematic and smectic ordering of homeotropically anchored uniaxial and biaxial hard rods in slit-like pores [24, 25]. In particular, we showed [24] that the nematic-smectic transition is suppressed due to the restricted geometry along the direction of the density modulation. In the present work we change our focus to the cylindrical confinement and consider planar anchoring. This system behaves very differently from the slit-like pore: Since the cylinder is infinite in the direction of the smectic density wave, there are no geometric restrictions and the nematic-smectic phase transition can survive in the cylindrical pore. Our study reveals that planar anchoring widens the stability window of the nematic phase and shrinks the region of smectic ordering in cylindrical pores. The case of homeotropic anchoring in cylindrical geometry involves topological restrictions that give rise to defects and is not considered

*Electronic address: vargasz@almos.uni-pannon.hu

†Electronic address: yuri@math.uc3m.es

‡Electronic address: enrique.velasco@uam.es

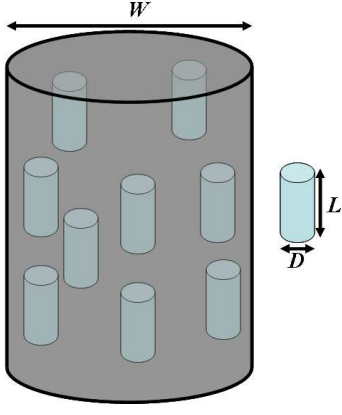


FIG. 1: Schematic of the confinement and the molecular model: W is the width of the cylindrical pore, and L and D are the length and the diameter of the hard cylinder particle, respectively.

here.

II. THEORY

We study the phase behaviour of a system of parallel hard cylinders confined in a cylindrical hard pore, as shown in Fig. 1. The molecular parameters are the length (L) and the diameter (D) of the cylinder. The particle orientations are taken to be parallel to the cylindrical pore, which is infinitely long but has a finite size in the perpendicular plane. Note that the width of the pore (W) must be larger than D . The appropriate thermodynamic function for studying confined fluids is the grand-potential density functional $\Omega[\rho]$ [26], which is given by

$$\beta\Omega[\rho] = \beta\mathcal{F}[\rho] - \int_V d\mathbf{r} \rho(\mathbf{r}) [\beta\mu - \beta V_{\text{ext}}(\mathbf{r})], \quad (1)$$

where $\beta = 1/kT$, k is Boltzmann's constant, T is temperature, \mathcal{F} is the Helmholtz free-energy functional, V is the volume of the pore, \mathbf{r} is the position vector of the rod, $\rho(\mathbf{r})$ is the local number density, and μ is the chemical potential. We attach a cylindrical coordinate frame to the centre of the pore. Let (R, ϕ, z) be the cylindrical coordinates of a position vector \mathbf{r} . The external potential due to the confinement, $V_{\text{ext}}(\mathbf{r})$, is considered to be hard, i.e. the surfaces of the cylinders have to be inside the pore. It takes the form

$$\beta V_{\text{ext}}(\mathbf{r}) = \begin{cases} \infty, & R > R_e \\ 0, & 0 \leq R \leq R_e, \end{cases} \quad (2)$$

where $R_e = (W - D)/2$ is the effective pore radius. The Helmholtz free energy, which is the sum of ideal and excess contributions ($\mathcal{F} = \mathcal{F}_{\text{id}} + \mathcal{F}_{\text{ex}}$), can be determined

from

$$\begin{aligned} \beta\mathcal{F}_{\text{id}}[\rho] &= \int_V d\mathbf{r} \rho(\mathbf{r}) \{ \log [\rho(\mathbf{r}) \Lambda^3] - 1 \}, \\ \beta\mathcal{F}_{\text{ex}}[\rho] &= -\frac{1}{2} \int_V d\mathbf{r}_1 \rho(\mathbf{r}_1) \int_V d\mathbf{r}_2 \rho(\mathbf{r}_2) f_{\text{M}}(\mathbf{r}_{12}), \end{aligned} \quad (3)$$

where Λ is the thermal wavelength, $f_{\text{M}}(\mathbf{r}_{12}) = \exp[\beta u(\mathbf{r}_{12})] - 1$ is the Mayer-function, $u(\mathbf{r}_{12})$ is the pair potential between two particles, and $\mathbf{r}_{12} = \mathbf{r}_1 - \mathbf{r}_2$. In the case of hard cylinders the Mayer-function can be written as $f_{\text{M}}(\mathbf{r}_{12}) = -\Theta(D - R)\Theta(L - z)$, where $\Theta(x)$ is the Heaviside step function. Note that the ideal contribution is exact, while the excess part is approximated at the level of Onsager second-virial theory [24]. To obtain the equilibrium density profile, the grand-potential functional has to be minimized with respect to the local density, i.e. $\delta\Omega/\delta\rho(\mathbf{r}) = 0$. Using Eqns. (1) and (3), one can easily show that the equilibrium profile $\rho(\mathbf{r})$ is given by the Euler-Lagrange equation

$$\rho(\mathbf{r}) = e^{\beta[\mu - V_{\text{ext}}(\mathbf{r})]} \times e^{\int_V d\mathbf{r}_1 \rho(\mathbf{r}_1) f_{\text{M}}(\mathbf{r} - \mathbf{r}_1)}. \quad (4)$$

As we focus our study on the structures of nematic and smectic phases in cylindrical confinement, the local density does not depend on the azimuthal angle ϕ , but only on R and z . Using the Mayer-function of hard cylinders and the external potential (2), the resulting Euler-Lagrange equation for $\rho(R, z)$, in the region where it is different from zero, is given by

$$\begin{aligned} \rho(R, z) &= e^{\beta\mu} \exp \left[- \int_{z-L}^{z+L} dz_1 \int_{\max(0, R-D)}^{\min(R_e, R+D)} dR_1 R_1 \right. \\ &\quad \left. \times \rho(R_1, z_1) \Phi_{\text{exc}}(R, R_1) \right], \end{aligned} \quad (5)$$

where

$$\Phi_{\text{exc}}(R_1, R_2) = \begin{cases} 2\pi, & R_{12}^+ < D, \\ 2 \cos^{-1}(t_{12}), & R_{12}^- \leq D \leq R_{12}^+, \\ 0, & R_{12}^- > D, \end{cases} \quad (6)$$

where we have defined $t_{12} = (R_1^2 + R_2^2 - D^2) / (2R_1 R_2)$, $R_{12}^- = |R_1 - R_2|$ and $R_{12}^+ = R_1 + R_2$. We have solved Eqn. (5) through the discretization of the local density, assuming periodicity along z axis, using a trapezoidal rule for the numerical integration and an iterative method. The discretization is performed as follows: $\rho_{ij} \equiv \rho(R_i, z_j)$, where i and j are integers that define the discrete set of points in the pore, $R_i = i\Delta R$, with $\Delta R = R_e/N_R$, $i = 0, \dots, N_R$, and $z_j = j\Delta z$, with $\Delta z = d/N_z$, $j = 0, \dots, N_z$. d is the period of the smectic phase along the z axis. In our calculations we used $\Delta z = 0.05L$ and $\Delta R = 0.01D$. The discrete version of the equation is solved for given values of chemical potential μ and smectic period d , and the average packing fraction and smectic order parameter are determined

from

$$\eta_{\text{av}} = \frac{2\pi}{dA_e} \int_0^d dz \int_0^{R_e} dR R \eta(R, z),$$

$$S = \frac{2\pi}{dA_e} \int_0^d dz \int_0^{R_e} dR R \eta(R, z) \cos\left(\frac{2\pi z}{d}\right), \quad (7)$$

where $\eta(R, z) = (\pi L D^2 / 4) \rho(R, z)$ is the local packing fraction, and $A_e = \pi R_e^2$ is the effective pore area. The integrals over z and R in Eqn. (7) (and in fact all integrals in the present calculation) are also computed using a trapezoidal rule. In the nematic phase the local density depends only on R , and

$$\rho(R) = e^{\beta\mu} \exp \left[-2L \int_{\max(0, R-D)}^{\min(R_e, R+D)} dR_1 R_1 \right. \\ \left. \times \rho(R_1) \Phi_{\text{exc}}(R, R_1) \right], \quad (8)$$

The smectic order parameter is zero for any solution $\rho(R)$ without z dependence, while it has a positive value for a smectic-like solution $\rho(R, z)$. We use the particle length L as a scaling parameter for the smectic period, $d^* = d/L$, and the z coordinate, $z^* = z/L$. The other scaling parameter is the particle diameter, D , which we use to make R and W dimensionless: $R^* = R/D$ and $W^* = W/D$. In the next section we present the nematic and smectic density profiles obtained from Eqns. (5) and (8) and determine the phase boundary of the nematic-smectic phase transition.

III. RESULTS AND DISCUSSION

A. Structure of the fluid inside the pore

In very narrow pores ($1 < W^* < 2$), there is no room for particles to overtake each other, and only nearest-neighbour interaction along z occurs. The phase behaviour of the confined hard cylinders becomes identical to that of the one-dimensional Tonks gas [27]. It is well-known that such a system does not exhibit a thermodynamic phase transition from fluid to crystal structures (note however that a very dense Tonks gas shows some changes from a fluid- to a solid-like structure, in the sense that the distance between the peaks of the positional distribution function is close to the average distance between neighboring particles; see the review of Giaquinta [28]). The present approximate theory does predict a continuous fluid-crystal transition (the one-dimensional ‘crystal’ corresponding to the smectic) at unrealistically high densities. Therefore one has to be cautious with the predictions of Onsager second-virial theory for high densities in very narrow pores.

In the nematic fluid the density profile is homogeneous for $1 < W^* < 2$ because in this case $\Phi(R_1, R_2) = 2\pi$ is a constant. The density profile derived from Eqn. (8) is

$$\rho = e^{-2LA_e\rho + \beta\mu}, \quad (9)$$

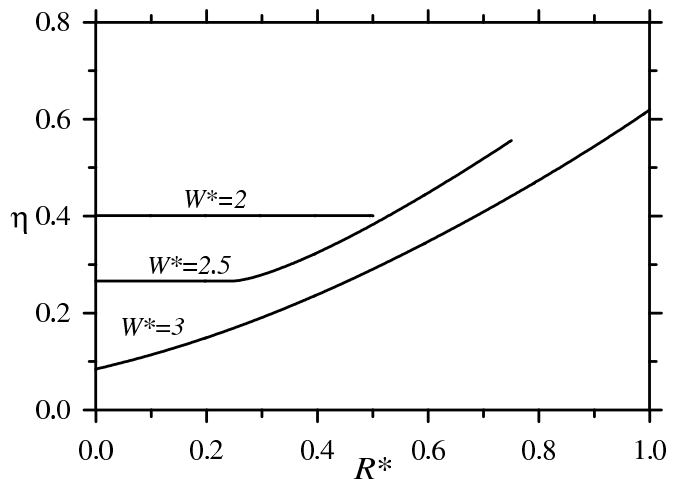


FIG. 2: Dimensional crossover from the one-dimensional Tonks gas to the three-dimensional fluid. Density profiles of hard cylinders in very narrow pores at $\eta_{\text{av}} = 0.4$.

which can be solved numerically for a given value of $\beta\mu$. This result is a consequence of the fact that the excluded volume of the particles, $V_{\text{exc}} = 2LA_e$ is always the same regardless of the location of the rod (either in the middle or at the wall of the pore).

This situation changes for $W^* > 2$, because more than one cylinder may fit into the pore in the same layer, i.e. overtaking can take place. The density profiles coming from the numerical solution of Eqn. (8) for $2 \leq W^* \leq 3$ are presented in Fig. 2. One can see that the density profile changes continuously from a homogeneous to an inhomogeneous distribution with increasing pore width. The reason why the density is constant in a small interval of radial distances from the pore centre for the case $W^* = 2.5$ is that particles staying in this region have the highest excluded volume and do not allow any particle to overtake them. At the same time, the density peak at the wall is due to the fact that particles can reach minimal excluded volume at the wall, which makes it possible to maximize the free volume available for the rest of the particles. This manifests very clearly at $W^* = 3$, where the fluid becomes completely inhomogeneous.

The structure of the fluid phase becomes even more interesting for wider pores, as shown in Fig. 3. The decreasing effect in excluded volume of the wall-particle interaction gives rise to oscillatory behaviour in the density profile. For $W^* = 3.8$ the strong adsorption tendency of the particles at the wall results in a depletion zone between the wall and the pore central region, while the density peak at the centre and that at the wall are comparable. The propagation of the oscillatory behaviour to a wider range of distances can be observed with increasing density at $W^* = 8$. For this pore width, the competition between wall-particle and particle-particle excluded-volume interactions results in a density minimum at the centre of the pore. The case $W^* = 20$ demonstrates

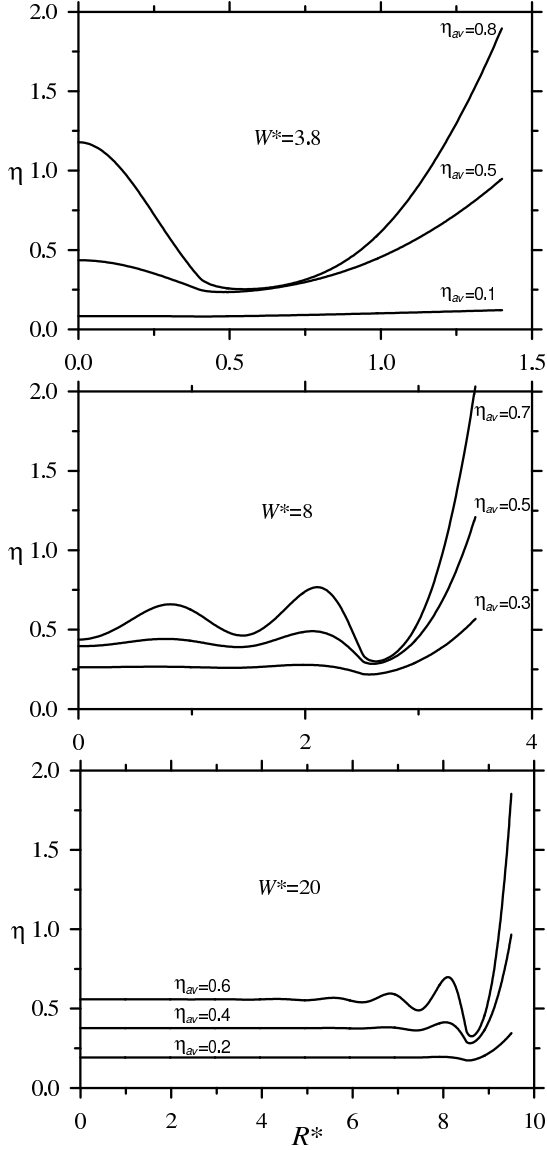


FIG. 3: Density profiles of hard cylinders as a function of average packing fraction η_{av} in three different pores.

that the effect of the wall decays exponentially from the wall to the pore centre, with a typical decaying length not exceeding $\sim 3 - 4D$ from the wall even at very high average packing fractions. Therefore the structure of a hard-cylinder fluid in very wide pores is altered only in the vicinity of the wall.

B. Nematic-smectic transition in the pore

The bulk system of parallel hard cylinders undergoes a continuous nematic-smectic phase transition. The nematic is a homogeneous fluid phase, while the smectic phase has a layered structure in the direction of the long

axis of the cylinder (one-dimensional solid). The equations for the transition density $\rho_{NS}^{(bulk)}$ and smectic period $d_{NS}^{(bulk)}$ of the bulk nematic-smectic transition are given by [23]

$$1 + 2\pi D^2 \rho_{NS}^{(bulk)} \frac{\sin(q_{NS}^{(bulk)} L)}{q_{NS}^{(bulk)}} = 0, \quad (10)$$

$$\frac{\partial}{\partial q_{NS}^{(bulk)}} \left[\frac{\sin(q_{NS}^{(bulk)} L)}{q_{NS}^{(bulk)}} \right] = 0 \quad (11)$$

where $q_{NS}^{(bulk)} = 2\pi/d_{NS}^{(bulk)}$ is the smectic wave number at the transition. These equations are obeyed by the values $\eta_{NS}^{(bulk)} \simeq 0.575$ and $d_{NS}^{(bulk)*} \simeq 1.398$, where $\eta_{NS}^{(bulk)} = (\pi L D^2 / 4) \rho_{NS}^{(bulk)}$ is the critical packing fraction. To determine the locus of the nematic-smectic transition points in the confined system, we add a smectic modulation to the fluid density as

$$\rho(R, z) = \rho_0(R) [1 + \epsilon(R) \cos(qz)], \quad (12)$$

where $\rho_0(R)$ is the solution of Eqn. (8) for a given $\beta\mu$ and $\epsilon(R)$ measures the amplitude of a small density modulation. After substitution of Eqn. (12) into Eqn. (5) and linearization in $\epsilon(R)$ of the exponential function, we obtain the following equation for $\epsilon(R)$:

$$\epsilon(R) + 2 \frac{\sin(qL)}{q} \int_{\max(0, R-D)}^{\min(R_e, R+D)} dR' R' \rho_0(R') \times \Phi_{exc}(R, R') \epsilon(R') = 0. \quad (13)$$

Note that Eqn. (13) reduces to the first of Eqns. (11) in the limit $W \rightarrow \infty$, where the local density and $\epsilon(R)$ become constant. The case of very narrow pores ($1 < W^* < 2$) is very similar to the bulk case, because it is possible to simplify Eqn. (13) to

$$1 + 2A_e \rho_{NS} \frac{\sin(q_{NS} L)}{q_{NS}} = 0, \quad (14)$$

where ρ_{NS} satisfies Eqn. (9). Comparison of the first of Eqns. (11) and (14) shows that $\eta_{NS} = (\pi D^2 / A_e) \eta_{NS}^{(bulk)}$. To numerically determine ρ_{NS} and q_{NS} for other cases where W is larger, it is useful to rewrite Eqn. (13) in discretised form, using the same space grid in radial direction R introduced before:

$$\sum_k A_{ik} \epsilon_k = 0, \quad (15)$$

where A_{ik} are the elements of a matrix A :

$$A_{ik} = \delta_{ik} + 2 \frac{\sin(qL)}{q} c_k R_k \rho_0(R_k) \Phi_{exc}(R_i, R_k). \quad (16)$$

Here $\{c_k, R_k\}$ are weights and roots for the trapezoidal-rule integration [note that the $\{c_k\}$ roots take account of the restricted integration interval in Eqn. (13), and give

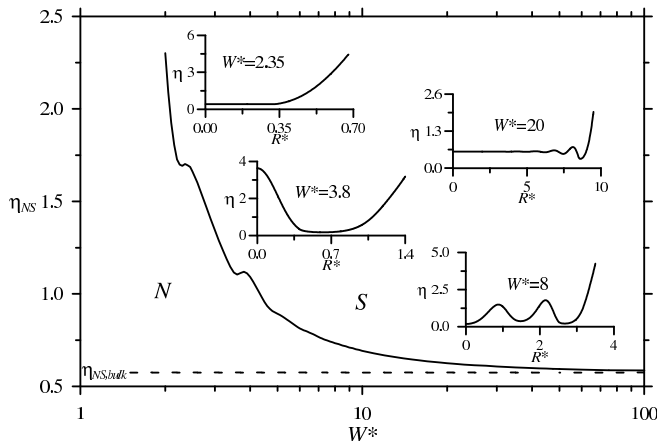


FIG. 4: Packing fraction η_{NS} of the nematic-smectic phase transition as a function of pore width (W). Insets show a few density profiles along the nematic-smectic transition curve. The dashed line indicates the packing fraction $\eta_{NS}^{(bulk)}$ of the bulk nematic-smectic phase transition. N and S denote the regions of nematic and smectic phase stability, respectively.

an A matrix which is band-diagonal]. At the nematic-smectic transition, the A matrix must obey the following two equations:

$$\det(A)|_{NS} = 0, \quad \left. \frac{\partial \det(A)}{\partial q} \right|_{NS} = 0, \quad (17)$$

which provide the transition density η_{NS} and period d_{NS} . The dimension of the A matrix depends on the values of R_e and ΔR . For all the cases studied, with the chosen values of R_e and ΔR , the number of points used result in accurate values for density and period.

One interesting outcome of Eqns. (17) is that the smectic period d_{NS} does not depend on the pore-width and is always equal to the bulk value, $d_{NS} = d_{NS}^{(bulk)} = 1.398L$. This is due to the fact that the R and z variables are decoupled in the Mayer function. However, as far as the transition density is concerned, there must be a dependence with pore width: in the bulk limit ($W \rightarrow \infty$), η_{NS} should go to the bulk value $\eta_{NS}^{(bulk)}$, while it should diverge when $W \rightarrow D^+$ (note that, as mentioned in the beginning of Section III A in connection with the isomorphism between the present model and Tonks gas, there should be no transition for $W \leq 2D$ and, as a consequence, the transition density should in fact diverge as $W \rightarrow 2D^+$). Therefore, the smectic phase should be destabilized with respect to the nematic phase with decreasing pore width.

The results of Eqn. (17) confirm this prediction. Fig. 4 shows that the destabilization of the smectic phase is weak for very wide pores, while in narrow pores it gets very strong as the contribution of the wall-particle excluded volume becomes comparable to that due to particle-particle excluded volume. This effect, although qualitatively correct, might be grossly overestimated by the present theory. For example, for $W^* = 5$, the increase in transition density exceeds the bulk value by

50% (note that the resulting density is quite close to the close-packing limit of hard cylinders while it is known from MC simulations of hard cylinders [19] that there is a large gap between the bulk nematic-smectic transition and the close-packing densities). Therefore it is clear that the predictions of our theory are correct but not quantitatively reliable for relatively narrow pores.

It is interesting to note the presence of damped oscillations in the nematic-smectic transition curve (see Fig. 4). This behavior is related to the commensuration between pore width and typical transverse particle distance when the former is changed. The density profiles along the nematic-smectic boundary shows very strong adsorption at the wall and depletion zones are also present at all pore widths. The structure in the pore centre is strongly affected by the pore diameter in narrow pores, since the structure generated at the surfaces may interfere coherently or incoherently in the central region. By contrast, in wide pores the density modulation does not reach the pore centre and rapidly decays to an almost constant value (even at the nematic-smectic phase boundary), the inhomogeneous density being restricted to a region of thickness $3 - 4D$ from the wall (see the inset of $W^* = 20$ in Fig. 4).

Finally we show in Fig. 5 the variation of the density profile of the smectic phase along the pore symmetry axis (with the value of the chemical potential chosen in the bulk smectic region). The upper curve shows the local density at the wall, $\eta(R_e, z)$, while the lower curve corresponds to the local density at the centre, $\eta(0, z)$. Note the smooth density modulations along the direction normal to the layers in both narrow and wide pores. In both cases the interstitial region ($z = d/2$) is not empty as the density is substantial even in the middle of the pore, i.e. the one-dimensional ordering is not strong along the layer normal. The average density profile along the pore axis (dashed curve) shows that the wall-particle excluded volume effect is very strong in a narrow pore, while it is marginal in a wide pore. This can be seen very clearly in the lower panel of Fig. 5, where the average density profile is just slightly different from the density profile in the pore centre. It can be also seen that the coupling in the ordering between normal and in-plane directions is weak in both cases. The insets of Fig. 5 show that the smectic order parameter goes smoothly to zero with decreasing packing fraction, i.e. the nematic-smectic phase transition is continuous even in cylindrical confinement.

IV. CONCLUSIONS

We have studied the effect of cylindrical confinement on the nematic and smectic phases of parallel hard rods using Onsager's second-virial theory. We found that the wall-rod interaction gives rise to inhomogeneous nematic and smectic structures, with strong adsorption taking place at the wall. The inhomogeneous packing of the rods gives rise to a decrease in the average excluded volume of

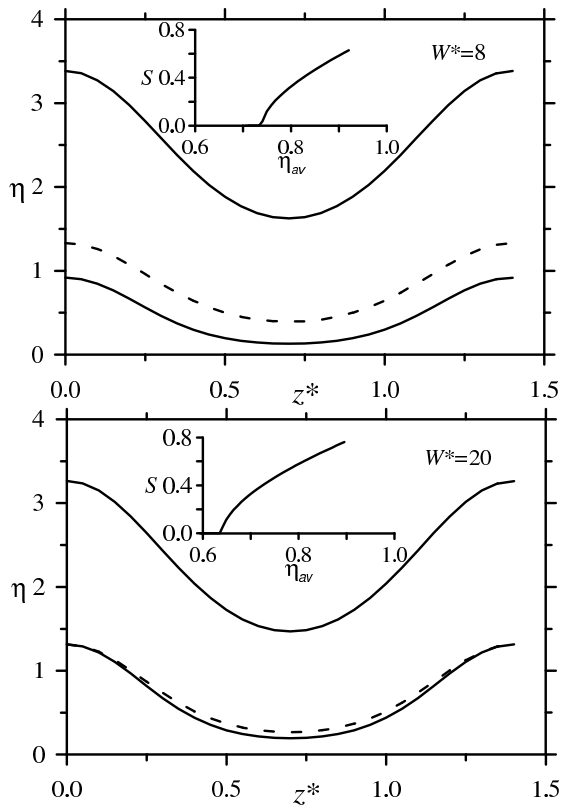


FIG. 5: Density profiles of the smectic phase along the main axis of the pore at the wall (upper curves) and in the centre of the pore (lower curves). Top panel: $W^* = 8$ and $\eta_{av} = 0.8$. Bottom panel: $W^* = 20$ and $\eta_{av} = 0.7$. The dashed curve is the average density profile along the main axis of the pore, $\eta(z) = (2\pi/A_e) \int_0^{R_e} dR R \eta(R, z)$. The insets show the smectic order parameter S as a function of average packing fraction η_{av} .

a particle, i.e. the free volume available for the particles in the pore can be increased substantially. In addition to this, the stability region of the smectic phase is shifted to higher densities with decreasing pore width. The observed nematic-smectic phase transition is continuous for any pore size. The reason for the destabilization of the smectic phase is that adding a one-dimensional spatial ordering to the inhomogeneous nematic phase cannot increase the packing entropy to the same extent as in the homogenous nematic phase. The transversal (in-plane) positional order is always present, while the longitudinal (out-of-plane) order takes place just above a critical density. In such a situation, the excluded volume gain from the longitudinal order cannot be as high as in the bulk nematic phase. It is worth mentioning that, in a fluid of Gay-Berne particles [15], the cylindrical confinement

also hinders the formation of the smectic phase.

Although qualitatively correct, the predictions of this theory may be in error for narrow pores. A way to improve the predictions (but certainly not the essential physics) is to use a Parsons-Lee scheme [29, 30], where the high-density terms of the diagrammatic expansion of the free-energy functional are approximated by those of a scaled fluid of hard spheres and the resulting series is resummed to give a density-renormalised free energy. This extended theory will, in the limit of small pore widths, give lower (and more realistic) values for the average packing fractions than those shown in Fig. 4.

We have not examined the stability of possible columnar and solid-like structures of the confined hard cylinders. The stabilization of columnar ordering is quite unrealistic because it does not exist in the bulk limit and the commensuration conflict between pore-size and particle diameter does not support the formation of packed two-dimensional lattices in the pore. However, the stabilization of columnar ordering cannot be excluded at some special pore widths, where the accommodation of the cylinders can be achieved efficiently in the pore. In very narrow pores, the existence of the nematic-smectic phase boundary is quite questionable and it may happen that a inhomogeneous nematic structure change continuously to a solid-like structure. The structure of such closely-packed phases may vary greatly with pore width, as is the case in cylindrically confined hard spheres [31, 32]. Our results clearly show that the nematic phase is the winner in the cylindrical confinement of parallel particles. As regards the freely rotating case, we can say that the stability window of the nematic phase is expected to be even wider because confinement enhances the orientational ordering of hard rods [13]. Therefore our study should be extended to the system of freely rotating hard rods in order to get a deeper understanding of the delicate interplay between the wall-rod and rod-rod interactions on the stability of isotropic, nematic, smectic and closed-packed structures.

Acknowledgments

SV acknowledges the financial support of the Hungarian State and the European Union under the TAMOP-4.2.2.A-11/1/KONV-2012-0071. Financial support from Comunidad Autónoma de Madrid (Spain) under the R&D Programme of Activities MODELICO-CM/S2009ESP-1691, and from MINECO (Spain) under grants FIS2010-22047-C01 and FIS2010-22047-C04 is also acknowledged.

[1] S. Ishihara, J. Display Technol. **1**, 30 (2005).

[2] P. Sheng, Phys. Rev. Lett. **37**, 1059 (1976).

- [3] R.-M. Marroum, G. S. Iannacchione, D. Finotello, and M. A. Lee, Phys. Rev. E **51**, 2743 (1995).
- [4] G. P. Sinha and F. M. Aliev, Phys. Rev. E **58**, 2001 (1998).
- [5] A. V. Kityk, M. Wolff, K. Knorr, D. Morineau, R. Lefort and P. Huber, Phys. Rev. Lett. **101**, 187801 (2008).
- [6] A. V. Kityk and P. Huber, Appl. Phys. Lett. **97**, 153124 (2010).
- [7] C. Grigoriadis, H. Duran, M. Steinhart, M. Kappl, H.-J. Butt and G. Floudas, ACS Nano **5**, 9208 (2011).
- [8] C. V. Cerclier, M. Ndao, R. Busselez, R. Lefort, E. Grelet, P. Huber, A. V. Kityk, L. Noirez, A. Schönhals and D. Morineau, J. Phys. Chem. C **116**, 18990 (2012).
- [9] W.-Y. Zhang, Y. Jiang, and J. Z.Y. Chen, Phys. Rev. Lett. **108**, 057801 (2012).
- [10] S. Calus, D. Rau, P. Huber and A. V. Kityk, Phys. Rev. E **86**, 021701 (2012).
- [11] R. van Roij, M. Dijkstra and R. Evans, Europhys. Lett. **49**, 350 (2000).
- [12] M. Dijkstra, R. van Roij and R. Evans, Phys. Rev. E **63**, 051703 (2001).
- [13] D. de las Heras, E. Velasco and L. Mederos, Phys. Rev. Lett. **94**, 017801 (2005).
- [14] Q. Ji, R. Lefort and D. Morineau, Chem. Phys. Lett. **478**, 161 (2009).
- [15] Q. Ji, R. Lefort, R. Busselez and D. Morineau, J. Chem. Phys. **130**, 234501 (2009).
- [16] H. Reich and M. Schmidt, J. Phys.: Condens. Matter **19**, 326103 (2007).
- [17] M. M. Pineiro, A. Galindo and A. O. Parry, Soft Matter **3**, 768 (2007),
- [18] L. Harnau and S. Dietrich, Phys. Rev. E **66**, 051702 (2002).
- [19] J. A. C. Veerman and D. Frenkel, Phys. Rev. A **43** 4334 (1991).
- [20] J. A. Capitán, Y. Martínez-Ratón and J. A. Cuesta, J. Chem. Phys. **128**, 194901 (2008).
- [21] L. Onsager, Ann. N. Y. Acad. Sci. **51**, 627 (1949).
- [22] G. J. Vroege and H. N. W. Lekkerkerker, Rep. Progr. Phys. **55**, 1241 (1992).
- [23] B. Mulder, Phys. Rev. A **35**, 3095 (1987); R. P. Sear and G. Jackson, J. Chem. Phys. **102**, 2622 (1995).
- [24] A. Malijevsky and S. Varga, J. Phys.: Condens. Matter, **22**, 175002 (2010).
- [25] S. Varga, Y. Martínez-Ratón and E. Velasco, Eur. Phys. J. E **32**, 89 (2010).
- [26] J. P. Hansen and I. R. McDonald, Theory of Simple Liquids, 2nd ed. (Academic Press, London, 1986).
- [27] L. Tonks, Phys. Rev. **50**, 955 (1936).
- [28] P.V. Giaquinta, Entropy **10**, 248 (2008).
- [29] J. D. Parsons, J. Chem. Phys. **19**, 1225 (1979).
- [30] S. D. Lee, J. Chem. Phys. **87**, 4972 (1987).
- [31] M. C. Gordillo, B. Martínez-Haya and J. M. Romero-Enrique, J. Chem. Phys. **125**, 144702 (2006); F. J. Durán-Olivencia and M. C. Gordillo, Phys. Rev. E **79**, 061111 (2009)
- [32] A. Mughal, H. K. Chan and D. Weaire, Phys. Rev. Lett. **106**, 115704 (2011).